



HAL
open science

Population Modeling of Influenza A/H1N1 Virus Kinetics and Symptom Dynamics

Laetitia Canini, Fabrice Carrat

► **To cite this version:**

Laetitia Canini, Fabrice Carrat. Population Modeling of Influenza A/H1N1 Virus Kinetics and Symptom Dynamics. *Journal of Virology*, 2010, 85 (6), pp.2764 - 2770. 10.1128/jvi.01318-10. hal-04629005

HAL Id: hal-04629005

<https://hal.science/hal-04629005>

Submitted on 28 Jun 2024

HAL is a multi-disciplinary open access archive for the deposit and dissemination of scientific research documents, whether they are published or not. The documents may come from teaching and research institutions in France or abroad, or from public or private research centers.

L'archive ouverte pluridisciplinaire **HAL**, est destinée au dépôt et à la diffusion de documents scientifiques de niveau recherche, publiés ou non, émanant des établissements d'enseignement et de recherche français ou étrangers, des laboratoires publics ou privés.

Updated information and services can be found at:
<http://jvi.asm.org/content/85/6/2764>

REFERENCES

These include:

This article cites 31 articles, 15 of which can be accessed free at: <http://jvi.asm.org/content/85/6/2764#ref-list-1>

CONTENT ALERTS

Receive: RSS Feeds, eTOCs, free email alerts (when new articles cite this article), [more»](#)

Information about commercial reprint orders: <http://journals.asm.org/site/misc/reprints.xhtml>
To subscribe to to another ASM Journal go to: <http://journals.asm.org/site/subscriptions/>

Population Modeling of Influenza A/H1N1 Virus Kinetics and Symptom Dynamics[∇]

Laetitia Canini^{1,2} and Fabrice Carrat^{1,2,3*}

UPMC Université Paris 06, UMR-S 707, Paris F-75012, France¹; Inserm, UMR-S 707, Paris F-75012, France²; and Assistance Publique Hôpitaux de Paris, Hôpital Saint Antoine, Paris F-75012, France³

Received 21 June 2010/Accepted 21 December 2010

Influenza virus kinetics (VK) is used as a surrogate of infectiousness, while the natural history of influenza is described by symptom dynamics (SD). We used an original virus kinetics/symptom dynamics (VKSD) model to characterize human influenza virus infection and illness, based on a population approach. We combined structural equations and a statistical model to describe intra- and interindividual variability. The structural equations described influenza based on the target epithelial cells, the virus, the innate host response, and systemic symptoms. The model was fitted to individual VK and SD data obtained from 44 volunteers experimentally challenged with influenza A/H1N1 virus. Infection and illness parameters were calculated from best-fitted model estimates. We predicted that the cytokine level and NK cell activity would peak at days 2.2 and 4.2 after inoculation, respectively. Infectiousness, measured as the area under the VK curve above a viral titer threshold, lasted between 7.0 and 1.3 days and was 15 times lower in participants without systemic symptoms than in those with systemic symptoms ($P < 0.001$). The latent period, defined as the time between inoculation and infectiousness, varied from 0.7 to 1.9 days. The incubation period, defined as the time from inoculation to first symptoms, varied from 1.0 to 2.4 days. Our approach extends previous work by including the innate response and providing realistic estimates of infection and illness parameters, taking into account the strong interindividual variability. This approach could help to optimize studies of influenza VK and SD and to predict the effect of antivirals on infectiousness and symptoms.

Viral shedding kinetics and symptom dynamics (SD) are often used to describe the natural course of infections. In influenza virus infection, virus kinetics (VK) is used as a surrogate for infectiousness, and parameters such as the latent period, the duration of infectiousness, and the generation time can be deduced directly from viral shedding data (13). The standard influenza virus kinetic pattern includes rapid exponential growth, peak viral load occurring 2 to 3 days after infection, and a decline toward virus undetectability over the following 3 days (5, 8, 10).

This kinetic pattern results from interactions between the virus, host target cells, and the immune system. During the first days of infection, the innate immune response, mediated by cytokines and natural killer (NK) cells, provides nonspecific defenses pending activation of adaptive responses (16). Cytokines have a protective role, but their levels also correlate with systemic symptom dynamics. In particular, interleukin 6 (IL-6) and alpha interferon (IFN- α) levels in nasal washing fluid are causally linked to viral titers, body temperature, mucus production, and symptom scores (20).

Nonlinear models have previously been used to characterize the kinetics of agents causing chronic infections, such as HIV (29), hepatitis B virus (28), and hepatitis C virus (27), and have proved useful both for explaining sustained replication and for studying the effect of antiviral drugs. Few nonlinear models of influenza have been published (4, 6, 17–19, 21, 24, 26, 31), and

only one used actual human data (3). The latter model was fitted to viral shedding data from six experimentally challenged subjects and was based on compartments describing target epithelial cells (infected or uninfected), the virus titer, and the interferon response.

We extended this model and used an original virus kinetics/symptom dynamics (VKSD) “population” approach to estimate infection parameters and to characterize the overall pattern and variability of influenza virus infection and illness. Our approach fits VK and SD simultaneously, using predicted (unobserved) cytokine and NK cell effects.

Data came from the experimental influenza virus infection of healthy volunteers who showed substantial variability in viral shedding and symptoms, with some individuals remaining asymptomatic (32). In the “population” approach, widely employed in pharmacokinetic/pharmacodynamic studies, the data are modeled with structural equations and a statistical model to capture the full intra- and interindividual variability of virus kinetics and symptoms.

MATERIALS AND METHODS

Design. We used data from five randomized, double-blind, placebo-controlled registration studies of zanamivir treatment of H1N1 influenza virus (NAIA1001, NAIA1002, NAIA1003, NAIA1004, and NAIA1010). The studies were conducted between 1993 and 1997 and involved experimentally challenged volunteers. All were approved by ethics committees, and the volunteers gave their written informed consent.

Volunteers were eligible for these studies if they were Caucasian men or women aged from 18 to 40 years, with serum hemagglutinin antibody titers of $\leq 1:8$ to the relevant virus strains. They were nonsmokers or smoked an average of less than 10 cigarettes per day and agreed not to smoke for the duration of the isolation period. They had normal pulmonary function, were within $\pm 30\%$ of their ideal weight for height, were using effective contraception (women), and were judged to be healthy based on medical history taking, physical examination,

* Corresponding author. Mailing address: Epidémiologie, Systèmes d'Information, Modélisation, UMR-S 707, Faculté de Médecine Saint Antoine, 27 Rue Chaligny, 75571 Paris, Cedex 12, France. Phone: 33 1 44 73 84 51. Fax: 33 1 44 73 84 53. E-mail: carrat@u707.jussieu.fr.

[∇] Published ahead of print on 29 December 2010.

routine laboratory investigations, screening electrocardiograms (ECGs), and the absence of lymphadenopathy.

The volunteers were challenged with 10^5 median (50%) tissue culture infective doses (TCID₅₀) of influenza A/Texas/91 (H1N1) virus intranasally and were monitored daily for the following 7 or 8 days. A sample for viral shedding kinetics analysis was taken from each volunteer 8 or 9 times. In four studies (48 subjects), sample collection took place on day 0 (D0) before the challenge, and then on D1, D2, D3, D4, D5, D6, D7, and D8; no D8 sample was collected in the fifth study (8 subjects). The following symptoms were noted: earache, runny nose, sore throat, coughing, sneezing, breathing difficulties, muscle ache, fatigue, headache, a feverish feeling, hoarseness, and chest discomfort. The intensity of each symptom was scored by the patient from 0 (none) to 3 (severe). The symptom data were collected twice a day, at 0800 and 2000 on the same days as the viral titer samples.

A systemic symptom score (range, 0 to 12) was constructed by summing the scores for muscle ache, fatigue, headache, and a feverish feeling. We focused on these systemic symptoms as they occurred first (8) and adequately delineated the incubation period. In addition, these symptoms are causally related to the cytokine level (20).

We also summed all the systemic symptom scores over the entire study period. Volunteers with total systemic symptom scores below 2 over the 7 or 8 days of follow-up were considered free of systemic symptoms.

On the whole, 56 volunteers were included in the placebo arms of these trials. For this study, we selected subjects who had virus-positive samples on at least one occasion after the challenge, leading us to exclude 12 volunteers who were considered to not have been infected as they did not shed virus.

Forty-four volunteers with a mean age of 22.7 ± 4.2 years (range, 18 to 35 years) were selected, of whom 35 (80%) were male. The mean body mass index (BMI) was 24.3 ± 3.5 kg/m² (range, 18.8 to 33.6 kg/m²).

The subjects were influenza virus positive for 1 to 8 days (at least), and the observed viral titer peak ranged from 0.75 to 9.5 log₁₀ (TCID₅₀/ml).

The observed systemic symptom scores ranged from 0 to 10 points, and systemic symptoms lasted between 0 and 8 days (or more). Six volunteers had no respiratory symptoms and no systemic symptoms and were thus considered totally asymptomatic. Maximal viral shedding did not correlate with the maximal systemic symptom score (Spearman's rho, -0.28; $P = 0.18$).

Viral shedding. Daily nasal washing fluid samples, first taken on the day before virus inoculation, were collected by introducing 5 ml of phosphate-buffered saline per nostril and allowing it to dwell for 10 to 15 s before the volunteer gently blew into a sterile container that was then transported to the laboratory for processing. Two milliliters of each sample was combined with 0.5 ml of concentrated virus transport medium. The residual sample was stored at -70°C until titration. Aliquots of 0.2 ml were inoculated on quadruplicate monolayers. Samples were incubated at 33 to 35°C for 14 days and examined for cytopathic effects every day. Negative controls were conducted each day. Titers were calculated from 10-fold dilutions of positive samples by the Karber method and expressed as TCID₅₀ per ml (14).

Modeling. (i) Population VKSD model. Population VKSD models were constructed with MONOLIX software version 3.1, and population parameters were estimated with the maximum likelihood method and the stochastic approximation expectation maximization algorithm (23). The two responses (viral shedding titer and systemic symptom score) were fitted simultaneously.

(ii) Structural VK model. This model extended the IFN compartmental model proposed by Baccam et al. (3) and used a set of ordinary differential equations. The compartments were uninfected target cells (T), infected but not yet virus-producing cells (I_1), productively infected cells (I_2), cytokines (F), natural killer (NK) cells, and infectious viral titers expressed in TCID₅₀/ml (V) (Fig. 1). Note that the cytokine compartment is taken "as a whole" and is not restricted to IFN as in the Baccam et al. model. Cytokine production was assumed to be directly proportional to the number of infected cells and was attributed either to infected cells themselves (30) or to activated macrophages and dendritic cells (2). The cytokine compartment included all cytokines, such as IFN- α and IL-6, that are causally linked to systemic symptoms, NK cell activation, and virus production (34).

The equations describing the VK model are as follows: $dT/dt = -\beta TV$; $dI_1/dt = \beta TV - kI_1$; $dI_2/dt = kI_1 - \delta I_2 - \tau I_2 NK$; $dF/dt = I_2 - \alpha F$; $dNK/dt = F - \xi NK$; and $dV/dt = pI_2(1 + \psi F) - cV$; where β is the target cell infection rate, k is the transition rate from I_1 to I_2 , δ is the mortality rate of infected cells, τ is the effect of NK cells on infected cells, α is the cytokine clearance, ξ is the mortality rate of NK cells, p is the rate of virus production by I_2 , ψ is the effect of cytokines on p , and c is the virus clearance. T_0 , the initial number of target cells in the upper respiratory tract, was set at 4×10^8 (3). We set the cytokine and NK cell

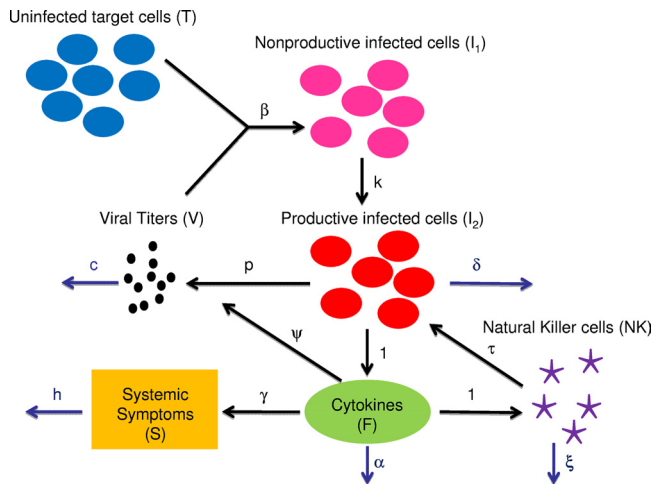


FIG. 1. Graphical presentation of the VKSD model. The free virus (V) infects target epithelial cells (T), which become infected cells not yet producing virus (I_1), before becoming productively infected cells (I_2). These latter cells produce free virus and lead to the production of cytokines (F), either directly or via activation of macrophages or dendritic cells. Cytokines reduce the virus production rate, activate natural killer (NK) cells and induce systemic symptoms (S). NK cells kill infected cells. The symbols above each arrow represent model parameters. Parameters between I_2 and F , or F and NK, were fixed at 1.

production rates to 1, as this changes only the units in which the early immune response is measured and does not lead to a loss of generality.

The average life span of infected cells is about 1 day (35), and δ was thus set at $k/(k - 1)$.

We defined the half-life of free virus (i.e., the time required for a 50% decline in the quantity of shed virus) as $\ln(2)/c$, the half-life of cytokines as $\ln(2)/\alpha$, and the half-life of NK cells as $\ln(2)/\xi$ (3, 36).

(iii) Structural SD model. Systemic symptoms were modeled as being dependent on the level of cytokines (20), as follows: $dS/dt = \gamma F - hS$, where γ is the rate at which systemic symptoms (S) appear and h is the rate of symptom resolution.

(iv) Modeling the different degrees of variability. In the population approach, each model parameter can be decomposed into a "population" parameter (a fixed effect) and an interindividual variability (IIV) parameter (a random effect). We illustrate this approach in a simple modeling example (Fig. 2). In our VKSD model, the IIV parameters were tested one by one to determine if they significantly improved the model. The three different error models (additive, multiplicative, and mixed) (12) were tested to model residual variability. The model was fitted for two responses: the viral titer and the systemic symptom score. The minimum value of the objective function ($-2 \log$ likelihood) was the main criterion used for model selection. Nested models were compared by using the likelihood ratio test (11). Model selection was also based on goodness-of-fit plots, and the precision of the parameter estimates, in terms of the relative standard error (RSE), was calculated as the standard deviation (STD) estimate divided by the parameter estimate.

Influenza infection and illness parameters. We estimated the latent period, infectiousness and its duration, the incubation period, and the generation time. The latent period is defined as the time during which a subject is infected but not yet infectious, while the duration of infectiousness is the average period for which an individual is capable of transmitting the infection; the incubation period is defined as the average time from infection to the appearance of symptoms of disease (1).

As the viral shedding titer above which a subject will enter the infectious period is unknown, we calculated the latent period, infectiousness, and the duration of infectiousness for various thresholds of viral shedding titers. The latent period was calculated as the time from inoculation to viral shedding exceeding a given threshold for the first time. Infectiousness was calculated as the area under the predicted VK curve (AUC) above the threshold (maximal infectiousness corresponding to the AUC calculated with no threshold), and the

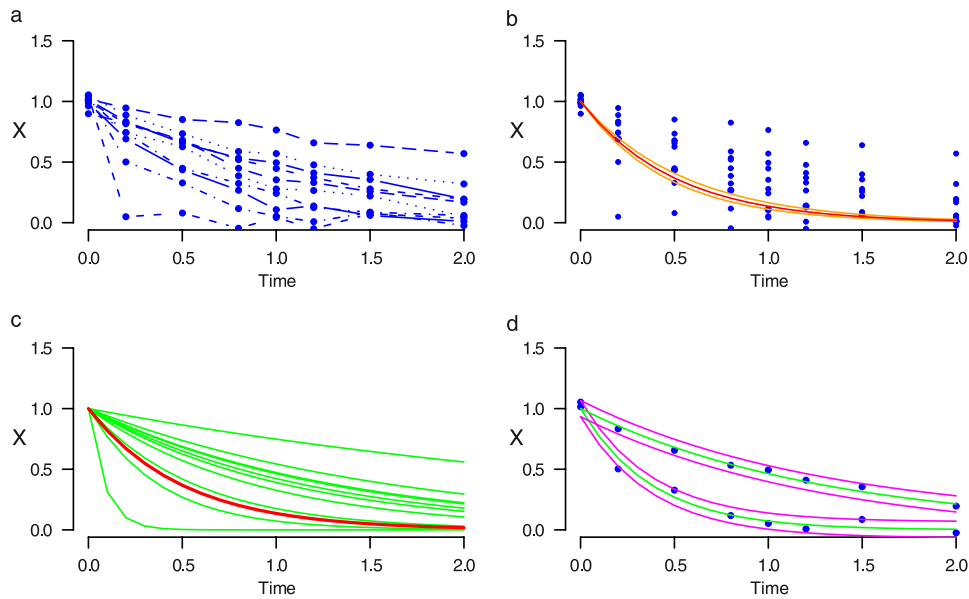


FIG. 2. Illustrative explanation of the population approach. We illustrate the statistical population approach with a simple monocompartmental model simulated on individuals ($i = 10$) and described by the equation $dX/dt = -kX$ [i.e., $X(t) = X(0) \times e^{-kt}$], with a single parameter, the elimination rate k . Parameter k was the population estimate but was assumed to vary across individuals such that k_i equals $k \exp(\eta_i)$, with η_i being normally distributed $(0, \omega^2)$. In the example, k equals 2 and ω equals 1, leading to an interindividual variability of 100%. To model residual variability, i.e., the difference between predicted and observed values, the following three different error models can be tested: additive [$X_i(t) = \hat{X}_i(t) + \varepsilon_1$], multiplicative [$X_i(t) = \hat{X}_i(t)(1 + \varepsilon_2)$], or mixed [$X_i(t) = \hat{X}_i(t)(1 + \varepsilon_2) + \varepsilon_1$], where ε_1 and ε_2 follow $N(0, \sigma_1^2)$ and $N(0, \sigma_2^2)$, respectively, and $\hat{X}_i(t)$ is the individual predicted value. (a) Simulated data for 10 subjects. (b) Population predictions (red line), the population confidence interval (orange lines), and the simulated data (blue dots) are shown. (c) Predicted individual curves (green). The population curve (red) is shown for information. (d) For two subjects, we present the individual prediction (green) and the prediction interval (magenta) obtained with the additive error model.

duration of infectiousness was defined as the period during which viral shedding exceeded the threshold.

The incubation period was calculated as the time from inoculation to the onset of a systemic symptom score of ≥ 1 in volunteers with systemic symptoms.

Finally, for the different thresholds, we calculated the generation time (T_g), an epidemiological parameter representing the mean interval between infection of a primary case and his/her secondary cases (33) and indicating the speed at which an epidemic spreads.

Assuming infectiousness to be proportional to the viral shedding titer, random contacts between infectious and susceptible individuals (i.e., homogeneous mixing) which do not depend on the viral shedding titer, T_g can be calculated (8, 15) as follows:

$$T_g = \frac{\int_0^{+\infty} t \times V(t) dt}{\int_0^{+\infty} V(x) dx}$$

We used the trapezoidal rule as a numerical integration method to compute the generation time from individually predicted VK curves.

RESULTS

Population VKSD model. The population VK and SD parameter estimates are shown in Table 1. The best results were obtained with an additive error model for both the VK and SD components. Interindividual variability on all parameters significantly improved the model.

The estimated average viral shedding titer increased sharply from day 1 and peaked 2.0 days after inoculation (Fig. 3), then fell rapidly to $1 \log_{10}$ (TCID₅₀/ml) between days 6 and 7. The

cytokine level and systemic symptom score showed roughly the same dynamic pattern, and their peaks lagged behind the viral titer peak by 0.2 and 0.4 days, respectively. The NK cell number peaked at 4.2 days but decayed slowly, remaining at 82% of the peak on day 8.

The half-life of free virus was 2.3 h (STD, 0.4 h). The average cytokine half-life was 9.1 h (STD, 1.8 h), and the average half-life of NK cells was 11.4 days (STD, 4.7 days).

Virus kinetics and symptom dynamics were highly variable across the volunteers, as shown in Fig. 4. Volunteers with the highest viral titers usually had the strongest predicted innate responses but not necessarily the highest symptom scores. Nineteen volunteers had no systemic symptoms, and these subjects had significantly lower peaks of viral shedding than volunteers with systemic symptoms ($P < 0.001$). The effect of cytokines on virus production and the virus clearance were significantly higher in volunteers without systemic symptoms than in volunteers with systemic symptoms (Table 2).

Influenza infection and illness parameters. The average latent period ranged from 0.4 days (STD, 0.3 days) to 1.5 days (STD, 0.6 days), depending on the chosen viral titer threshold (Fig. 5). In the same way, infectiousness lasted 1.3 days (STD, 0.8 days) at a threshold of $4 \log_{10}$ (TCID₅₀/ml) and 7.0 days (STD, 2.1 days) when no threshold was applied. In the latter case, 95% of the total amount of infectiousness was concentrated between day 1.2 and day 3.9 after inoculation. The incubation period was 1.9 days on average (STD, 0.7 days) and ranged from 0.9 to 4.5 days.

The average generation time was 2.1 days (STD, 1.0 day),

TABLE 1. Population VKSD parameter estimates and their precision^a

Parameter	Parameter description	Unit	Estimates (% RSE)	% IIV (% RSE)
β	Infection rate	$(\text{TCID}_{50}/\text{ml})^{-1} \cdot \text{day}^{-1}$	3.0×10^{-5} (18)	74 (19)
k	Transition rate from non productive to productive infected cells	Day^{-1}	2.8 (7)	28 (23)
τ	Effect of NK cells on infected cells		3.8×10^{-6} (49)	126 (36)
α	IFN clearance rate	[F]/day	1.82 (20)	111 (14)
ξ	Mortality rate of NK cells		0.061 (41)	114 (33)
p	Virus production rate	$\text{TCID}_{50}/\text{ml} \cdot \text{day}^{-1}$	0.043 (16)	60 (22)
c	Virus clearance rate	Day^{-1}	7.1 (17)	91 (15)
ψ	Effect of cytokines on virus production rate (p)	$[F]^{-1}$	2.4×10^{-7} (145)	778 (14)
V_0	Initial no. of viruses	$\text{TCID}_{50}/\text{ml}$	0.50 (13)	67 (15)
γ	Rate characterizing systemic symptoms	Symptom score point $\cdot \text{day}^{-1}$	2.2×10^{-6} (34)	78 (37)
h	Systemic symptom resolution rate	Day^{-1}	6.1 (26)	64 (40)
ϵ_V	Additive part of the model error for the viral titer	$\text{TCID}_{50}/\text{ml}$	1.2 (5)	
ϵ_S	Additive part of the model error for systemic symptoms	Symptom score point	0.59 (3)	

^a The estimates column provides the population fixed effect parameters or “average value of the parameter in the population” with their precision of estimation (relative standard error [RSE] as a percentage), while the IIV column represents the predicted interindividual variability for each parameter in the population and is shown along with its own precision of estimation.

while the times computed from individual predictions ranged from 1.2 to 6.2 days (Fig. 5).

Infectiousness was on average 14 to 16 times lower in volunteers without systemic symptoms than in volunteers with systemic symptoms (Fig. 5). The latent period was 0.2 days longer with the 0.5 log₁₀ (TCID₅₀/ml) threshold (Mann-Whitney test; $P = 0.045$), and the generation time was 1 day longer (Mann-Whitney test; $P = 0.002$) in subjects without systemic symptoms than in volunteers with systemic symptoms. However, regardless of the threshold, no significant difference in the duration of infectiousness was found between subjects with and without systemic symptoms.

DISCUSSION

We used an original model to characterize influenza virus shedding kinetics and symptom dynamics. This model offers a mechanistic approach to influenza infection and illness and an overall view of the disease time course. Relative to previous work, our approach comprises three novelties: influenza infection and illness were fitted simultaneously, the innate immune response was modeled and predicted, and we used a statistical population approach which contributes to the description and

explanation of different levels of variability, including interindividual variability. We also characterized major influenza infection and illness parameters. Our model parameter estimates for virus kinetics were of the same order as those found in other studies. The infection rate, β , was 2.7×10^{-5} to 3.2×10^{-5} $(\text{TCID}_{50}/\text{ml})^{-1} \cdot \text{days}^{-1}$ (3); the virus clearance, c , was 3.0 to 5.2 days^{-1} (3, 26); and we found 3.0×10^{-5} $(\text{TCID}_{50}/\text{ml})^{-1} \cdot \text{days}^{-1}$ (95% confidence interval [CI], 1.4×10^{-5} to 4.6×10^{-5}) and 7.1 days^{-1} (95% CI, 3.6 to 11), respectively. The average lifetime of infected cells was fixed at 1 day, as overfitting occurred when this parameter was estimated. The use of other lifetimes (12 h to 4 days) did not modify the main findings. The VK and SD curves were also consistent with those obtained in a previous study (8) in which the viral titer and systemic symptoms peaked on day 2. However, ours is the first study to quantify the interindividual variability of parameters describing viral shedding and symptoms. We showed that some of these parameters were highly variable across individuals, such as parameter ψ (the effect of cytokines on the virus production rate), while others were relatively constant across individuals, such as parameter k (the transition rate from I_1 to I_2).

As we had no data on cytokine or cellular responses, we designed the innate response compartments as a “black box,” representing the pooled cytokine response, and an NK cell compartment. We predicted that the cytokine level peaked at 2.2 days and had a half-life of 9.1 h. This pattern was similar to the IL-6 and IFN- α kinetics observed in a volunteer challenge study of influenza virus (20). The NK cell kinetics was in line with that found in a study of young subjects with Epstein-Barr virus infection (36). Our model does not take into account the adaptive immune response, as the early adaptive immune response, and particularly cytotoxic T lymphocyte destruction of virus-infected cells, would tend to appear a certain time after infection (nearly 5 days) and would peak later (between 9.5 to 11 days) (7). The adaptive response is unlikely to have a marked effect on the observed kinetics during the first days of infection.

The model predictions were then used to calculate several influenza virus infection and illness parameters. We arbitrarily

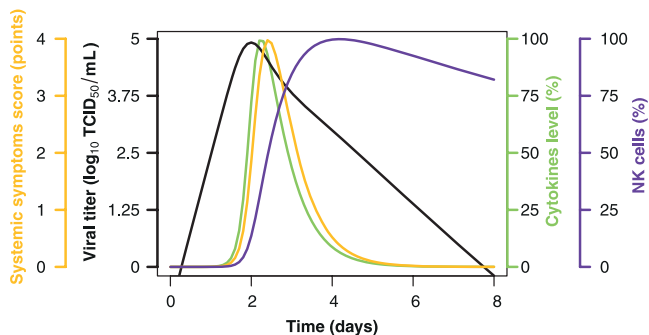


FIG. 3. Population predictions of viral titer (black), cytokines (green), and NK cell (purple) kinetics and systemic symptom intensity (orange) dynamics. The cytokine and NK cell kinetics were scaled in proportion to their maximum values.

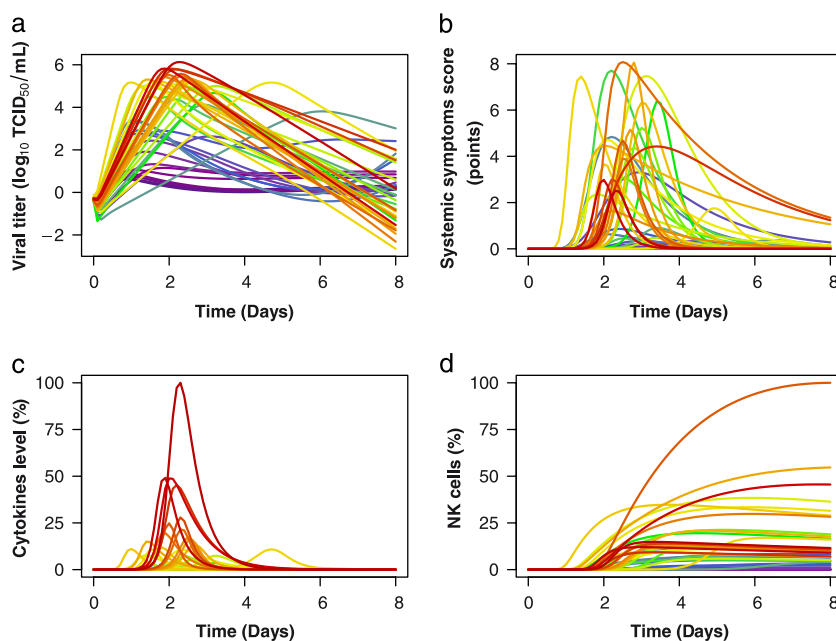


FIG. 4. Individual predictions of the viral titer (a), cytokines (c), and NK cell (d) kinetics and systemic symptom dynamics (b). The curves are ordered from the lowest peak viral titer (dark blue) to the highest (red). The order of the cytokines and NK cells peaks roughly follows that of the viral titers, contrary to the order of the peak systemic symptom scores.

those viral titer thresholds to distinguish between infectious and noninfectious individuals, as there is no clear boundary. We deduced from these thresholds a series of values for infectiousness, its duration, and the latent period. These parameter values were consistent with the results of previous studies (8, 9, 13, 25). The generation time was calculated assuming (i) infectiousness proportional to the viral titer, thus ignoring other key factors contributing to virus transmissibility, such as respiratory symptoms; and (ii) homogeneous random contacts independent of viral shedding. Our estimated generation time (2.1 days) was consistent with the values obtained in a meta-analysis of volunteer challenge studies (8) and with epidemiological data (13) but showed increased variability (range, 1.2 to 6.2 days), which may be important from an epidemiological standpoint. We found that participants without systemic symptoms were on average 15 times less infectious than participants with systemic symptoms, confirming and extending the results of a study of naturally acquired infection in which asymptomatic subjects had lower viral titer peaks than symptomatic subjects (22). We believe that this result is particularly important, as poorly symptomatic individuals who go undiagnosed are poorly infectious and would not markedly influence the effec-

tiveness of interventions (antivirals, isolation, etc.) aimed at controlling epidemics.

Our study has two main limitations. First, the analysis was based on a relatively homogeneous population, and second, the data came from experimental rather than naturally acquired infection. The applicability of our model to the natural infection depends on the pathogenicity of the virus used to challenge the volunteers, as well as preexisting immunity and the relevance of the challenge method to natural influenza virus acquisition (8). We believe that these issues are unlikely to affect the validity of our modeling approach: the viral shedding data and the rate of symptomatic infection, as well as the estimated infection and illness parameters, are consistent with the results of studies based on epidemiological data (13, 25).

Our findings have several important implications. First, similar models could be used to predict the time course of respiratory symptoms in influenza, thereby providing more realistic estimates of infectiousness by taking into account the high interindividual variability. Second, our approach could be used to predict the effect of antiviral treatment on infectiousness and symptoms. Finally, this approach might

TABLE 2. Differences in mean individual VKSD parameters between volunteers with and without systemic symptoms

Parameter	Parameter description	Unit	Systemic symptoms	No systemic symptoms	<i>P</i>
<i>p</i>	Virus production rate	TCID ₅₀ /ml · day ⁻¹	0.047	0.038	0.009
<i>ψ</i>	Effect of cytokines on virus production rate (<i>p</i>)	[<i>F</i>] ⁻¹	7.1 × 10 ⁻⁶	1.7 × 10 ⁻³	0.0001
<i>c</i>	Virus clearance rate	Day ⁻¹	7.6	10.3	0.03
<i>γ</i>	Rate characterizing systemic symptoms	Symptom score point · day ⁻¹	2.6 × 10 ⁻⁶	2.0 × 10 ⁻⁶	0.012

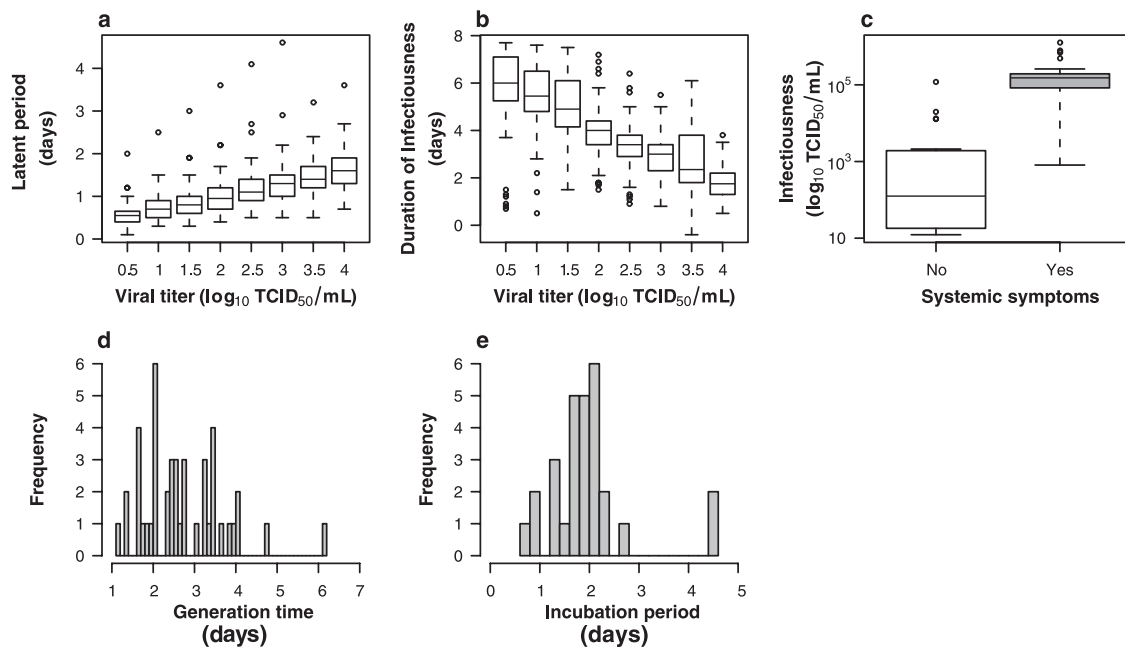


FIG. 5. Distribution of individual infection and illness parameters for the latent period (a) and infectiousness duration (b) computed for eight viral titer thresholds (0.5, 1, 1.5, 2, 2.5, 3, 3.5, and 4 log₁₀ [TCID₅₀/mL]), infectiousness (white, absence of systemic symptoms; gray, presence of systemic symptoms) (c), generation time (d), and incubation period (e).

help to optimize the design of future influenza VK and VKSD studies with respect to the necessary number of participants and samples.

ACKNOWLEDGMENTS

We thank J. P. Paccioni, S. Courcier, and S. Muller from Glaxo-SmithKline and I. Morer and P. Maison Neuve from the French Medicines Agency (AFSSAPS) for kindly providing the data used in this paper. We thank David Young, Marie-Lise Gougeon (Institut Pasteur, Paris, France), Béhazine Combadière (INSERM, Paris, France), and Brigitte Autran (Université Paris 06 and INSERM, Paris, France) for their advice on the manuscript.

This work was supported by a grant from the European Union FP7 project FLUMODCONT (no. 20160) and by a grant from the French Ministère de l'Enseignement Supérieur et de la Recherche.

REFERENCES

1. Anderson, R. M., and R. M. May. 1982. Directly transmitted infections diseases: control by vaccination. *Science* **215**:1053.
2. Asselin-Paturel, C., and G. Trinchieri. 2005. Production of type I interferons: plasmacytoid dendritic cells and beyond. *J. Exp. Med.* **202**:461–465.
3. Baccam, P., C. Beauchemin, C. A. Macken, F. G. Hayden, and A. S. Perelson. 2006. Kinetics of influenza A virus infection in humans. *J. Virol.* **80**:7590–7599.
4. Beauchemin, C., J. Samuel, and J. Tuszynski. 2005. A simple cellular automaton model for influenza A viral infections. *J. Theor. Biol.* **232**:223–234.
5. Bell, D. M. 2006. Non-pharmaceutical interventions for pandemic influenza, international measures. *Emerg. Infect. Dis.* **12**:81–87.
6. Bocharov, G. A., and A. A. Romanyukha. 1994. Mathematical model of antiviral immune response. III. Influenza A virus infection. *J. Theor. Biol.* **167**:323–360.
7. Brown, D. M., E. Roman, and S. L. Swain. 2004. CD4 T cell responses to influenza infection. *Semin. Immunol.* **16**:171–177.
8. Carrat, F., et al. 2008. Time lines of infection and disease in human influenza: a review of volunteer challenge studies. *Am. J. Epidemiol.* **167**:775–785.
9. Cauchemez, S., F. Carrat, C. Viboud, A. J. Valleron, and P. Y. Boelle. 2004. A Bayesian MCMC approach to study transmission of influenza: application to household longitudinal data. *Stat. Med.* **23**:3469–3487.
10. Cowling, B. J., et al. 2010. Comparative epidemiology of pandemic and seasonal influenza A in households. *N. Engl. J. Med.* **362**:2175–2184.

11. Cox, D. R., and D. V. Hinkley. 1997. *Theoretical statistics*. Chapman & Hall, London, United Kingdom.
12. Davidian, M., and D. M. Giltinan. 1995. *Nonlinear models for repeated measurement data*. Chapman & Hall/CRC Press, London, United Kingdom.
13. Ferguson, N. M., et al. 2005. Strategies for containing an emerging influenza pandemic in Southeast Asia. *Nature* **437**:209–214.
14. Finney, D. J. 1964. The Spearman-Kärber method, p. 524–530. *In* *Statistical methods in biological assay*. Charles Griffin and Co., London, United Kingdom.
15. Fraser, C., S. Riley, R. M. Anderson, and N. M. Ferguson. 2004. Factors that make an infectious disease outbreak controllable. *Proc. Natl. Acad. Sci. U. S. A.* **101**:6146.
16. French, A. R., and W. M. Yokoyama. 2003. Natural killer cells and viral infections. *Curr. Opin. Immunol.* **15**:45–51.
17. Hancioglu, B., D. Swigon, and G. Clermont. 2007. A dynamical model of human immune response to influenza A virus infection. *J. Theor. Biol.* **246**:70–86.
18. Handel, A., I. M. Longini, Jr., and R. Antia. 2007. Neuraminidase inhibitor resistance in influenza: assessing the danger of its generation and spread. *PLoS Comput. Biol.* **3**:e240.
19. Handel, A., I. M. Longini, Jr., and R. Antia. 2010. Towards a quantitative understanding of the within-host dynamics of influenza A infections. *J. R. Soc. Interface* **7**:35–47.
20. Hayden, F. G., et al. 1998. Local and systemic cytokine responses during experimental human influenza A virus infection. Relation to symptom formation and host defense. *J. Clin. Invest.* **101**:643–649.
21. Larson, E. W., J. W. Dominik, A. H. Rowberg, and G. A. Higbee. 1976. Influenza virus population dynamics in the respiratory tract of experimentally infected mice. *Infect. Immun.* **13**:438–447.
22. Lau, L. L., et al. 2010. Viral shedding and clinical illness in naturally acquired influenza virus infections. *J. Infect. Dis.* **201**:1509–1516.
23. Lavielle, M. 2005. MONOLIX (MODèles NON Linéaires à effets mixtes). The MONOLIX Group, Orsay, France.
24. Lee, H. Y., et al. 2009. Simulation and prediction of the adaptive immune response to influenza A virus infection. *J. Virol.* **83**:7151–7165.
25. Longini, I. M., Jr., et al. 2005. Containing pandemic influenza at the source. *Science* **309**:1083–1087.
26. Miao, H., et al. 2010. Quantifying the early immune response and adaptive immune response kinetics in mice infected with influenza A virus. *J. Virol.* **84**:6687–6698.
27. Neumann, A. U., et al. 1998. Hepatitis C viral dynamics in vivo and the antiviral efficacy of interferon-alpha therapy. *Science* **282**:103–107.
28. Nowak, M. A., et al. 1996. Viral dynamics in hepatitis B virus infection. *Proc. Natl. Acad. Sci. U. S. A.* **93**:4398–4402.

29. **Perelson, A. S., A. U. Neumann, M. Markowitz, J. M. Leonard, and D. D. Ho.** 1996. HIV-1 dynamics in vivo: virion clearance rate, infected cell life-span, and viral generation time. *Science* **271**:1582–1586.
30. **Pichlmair, A., and C. Reis e Sousa.** 2007. Innate recognition of viruses. *Immunity* **27**:370–383.
31. **Saenz, R. A., et al.** 2010. Dynamics of influenza virus infection and pathology. *J. Virol.* **84**:3974–3983.
32. **Samson, A., M. Lavielle, and F. Mentré.** 2006. Extension of the SAEM algorithm to left-censored data in nonlinear mixed-effects model: application to HIV dynamics model. *Comput. Stat. Data Analysis* **51**:1562–1574.
33. **Svensson, A.** 2007. A note on generation times in epidemic models. *Math Biosci.* **208**:300–311.
34. **White, M. R., M. Doss, P. Boland, T. Tecle, and K. L. Hartshorn.** 2008. Innate immunity to influenza virus: implications for future therapy. *Expert Rev. Clin. Immunol.* **4**:497–514.
35. **Zdanov, V. M., and A. G. Bukrinskaja.** 1969. Myxoviruses reproduction. *Medicina*, Moscow, Russia.
36. **Zhang, Y., et al.** 2007. In vivo kinetics of human natural killer cells: the effects of ageing and acute and chronic viral infection. *Immunology* **121**:258–265.